

Correlation effects in the electronic structure of the Ni-based superconducting KNi_2S_2 Feng Lu,¹ Wei-Hua Wang,² Xinjian Xie,³ and Fu-Chun Zhang^{1,4}¹*Department of Physics and Center for Theoretical and Computational Physics, University of Hong Kong, Hong Kong, China*²*Department of Electronics and Tianjin Key Laboratory of Photo-Electronic Thin Film Devices and Technology, Nankai University, Tianjin, China*³*School of Materials and Engineering, Hebei University of Technology, Tianjin, China*⁴*Department of Physics, Zhejiang University, Hangzhou, China*

(Received 4 February 2013; revised manuscript received 13 March 2013; published 22 March 2013)

The density functional theory (DFT) plus Gutzwiller variational method is used to investigate the ground-state physical properties of the newly discovered superconducting KNi_2S_2 . Five Ni-3*d* Wannier-orbital bases are constructed with DFT, to combine with local Coulomb interaction to describe the normal-state electronic structure of the Ni-based superconductor. The band structure and the mass enhancement are studied based on a multiorbital Hubbard model by using the Gutzwiller approximation method. Our results indicate that the correlation effects lead to the mass enhancement of KNi_2S_2 . Different from the band structure calculated from the DFT results, there are three energy bands across the Fermi level along the *X-Z* line due to the existence of the correlation effects, which induces a very complicated Fermi surface along the *X-Z* line. We have also investigated the variation of the quasiparticle weight factor with hole or electron doping and find that the mass enhancement character has been maintained with the doping.

DOI: [10.1103/PhysRevB.87.115131](https://doi.org/10.1103/PhysRevB.87.115131)

PACS number(s): 74.20.Pq, 71.15.Mb

I. INTRODUCTION

The discovery of the second class of high transition temperature superconductors in $\text{LaFeAsO}_{1-x}\text{F}_x$ ¹ has stimulated great interest in the study of iron pnictides. Over the past five years, many iron-based compounds have been reported to show superconductivity after doping or under high pressure,¹⁻⁴ and the superconducting (SC) transition temperature exceeds 50 K in $\text{RFeAsO}_{1-x}\text{F}_x$ (*R* = rare-earth atoms).⁵ Recently, one family, AFe_2Se_2 (*A* = K, Rb, or Tl) compounds, with the ThCr_2Si_2 -type crystal structure, such as $\text{K}_y\text{Fe}_2\text{Se}_2$ ⁶ and $(\text{Tl,K})_y\text{Fe}_{2-x}\text{Se}_2$,^{7,8} have been found to become superconductors at about 30 K. Different from other crystal structures of the iron-based superconductors, these compounds AFe_2Se_2 (*A* = K, Rb, or Tl) have many unique physical properties, such as the absence of a hole-like Fermi surface (FS) in $\text{K}_{0.8}\text{Fe}_{1.7}\text{Se}_2$ ⁹ and the intrinsic $\sqrt{5} \times \sqrt{5}$ Fe vacancy superstructure in $\text{K}_{0.8}\text{Fe}_{1.6}\text{Se}_2$.¹⁰⁻¹² Thus, searching for superconductors with the ThCr_2Si_2 -type crystal structure has become one of the interesting topics in condensed matter physics.^{13,14}

Very recently, a novel group of superconductors with ThCr_2Si_2 -type crystal structure, KNi_2A_2 (*A* = S, Se), have been discovered,^{15,16} which has stimulated great interest in the study of their physical properties.¹⁷ The experiments show that the Ni-based superconductor exhibits a rich and unusual electronic and structural phase diagram.^{15,16} For example, based on high-resolution synchrotron x-ray diffraction and time-of-flight neutron scattering experiments, James *et al.* have found that the mixed-valence compound KNi_2S_2 displays a number of highly unusual structural transitions and presents charge density wave fluctuations.¹⁶ Specific-heat measurement reveals that KNi_2S_2 exhibits the correlated behavior at low temperature with an enhanced effective electron mass $m^* = 11m_b$ to $24m_b$. Below $T_c = 0.46$ K, KNi_2S_2 becomes superconducting without the partial substitution of K or Ni deficiency.¹⁶ As discussed above, the Ni-based superconductor

KNi_2S_2 has a crystal structure similar to that of the iron-based superconductor AFe_2S_2 compound. However, there are also many differences between these two kinds of compounds. For example, the localized magnetism is absent in the Ni-based superconductor KNi_2S_2 .¹⁶ Thus, it is critical to understand the electronic structures of the parent ANi_2S_2 compounds at first in order to investigate the mechanism of superconductivity in this material.

In this paper, we have performed first-principles electronic structure calculations on KNi_2S_2 . To overcome the problem of dealing with Coulomb interaction in density functional theory (DFT) calculation, we use DFT plus the Gutzwiller variational approach to investigate this typical correlated material. This method has proved to be effective in dealing with Coulomb interaction and has been widely applied to strongly correlated systems.^{18,19} The calculation shows that KNi_2S_2 is a kind of multiorbital system with five Ni-3*d* orbital near the Fermi level. Our results indicate that the correlation effects of the 3*d* local electrons lead to mass enhancement of KNi_2S_2 . This behavior is always present with hole or electron doping, which is in good agreement with the experimental results.¹⁶ The correlation effect is not only presented by the narrowing of the bandwidth, but also by the change of the FS near the high symmetry line. In the DFT calculation, there are two bands across the *X-Z* line. Actually, there are three electron bands across the Fermi level along the *X-Z* line, which induce a very complicated FS structure along the *X-Z* line. The relationship among the quasiparticle weight factors of the different orbitals is also discussed in this paper.

II. MODEL AND METHOD

The plane wave basis method has been used in our calculation.²⁰ The generalized gradient approximation (GGA) was adopted for the exchange-correlation potentials.²¹ We used the ultrasoft pseudopotentials to model the electron-ion interactions.²² The kinetic energy cutoff and the charge density

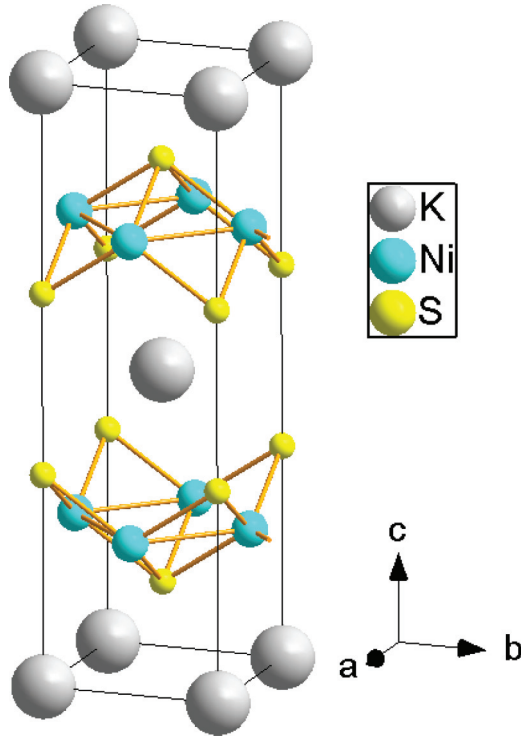


FIG. 1. (Color online) KNi_2S_2 with the ThCr_2Si_2 -type structure.

cutoff were taken as 800 and 6400 eV, respectively. A mesh of $18 \times 18 \times 9$ k points was used to perform the Brillouin zone integration. KNi_2S_2 has ThCr_2Si_2 -type structure [space group $I4/mmm$ (No. 139, $Z = 1$)] and each unit cell contains two formula units, as shown in Fig. 1. In our calculation, the

structure parameters optimized by the energy minimization, $a = 3.809 \text{ \AA}$, $c = 12.676 \text{ \AA}$, and $z(\text{S}) = 0.346$, were adopted, which are in good agreement with the experimental values $a = 3.779 \text{ \AA}$, $c = 12.714 \text{ \AA}$, and $z(\text{S}) = 0.35$ determined by synchrotron x-ray powder diffraction.¹⁶ Since the GGA cannot describe the Coulomb interaction adequately, in order to take into account more explicitly the correlated effects of the d electrons, we have performed the Gutzwiller variational approach to deal with the Coulomb interaction.

III. RESULTS AND DISCUSSION

We first present the electronic structure of KNi_2S_2 by DFT calculation. The corresponding band structures and FS are given in Fig. 2(a) and Fig. 2(b), respectively. Similar to the iron-based superconductor,^{23–28} there are several bands across the Fermi level, which indicates that KNi_2S_2 is a kind of multiorbital superconducting system. The multiorbital character can also be seen from the complicated FS sheets. As shown in Fig. 2(b), there is a large hole-like FS around the Γ point, two 2D-cylinder-like ones around the corners of the Brillouin zone, and a very complicated pocket at the middle of the four boundaries of the Brillouin zone. As mentioned above, the structure of the FS is very complicated due to the multiorbital characters, which implies that the KNi_2S_2 should be a kind of multiple-gap superconductor similar to the iron-based superconductor, in contrast to the single-orbital copper-based superconductors.

To investigate the orbital characters near the FS, the corresponding density of states (DOS) and the projected density of states (PDOS) of KNi_2S_2 are plotted in Fig. 3. The basic shape of the DOS and PDOS is very similar to that of AFe_2Se_2 .²⁹ However, the position of the Fermi energy is

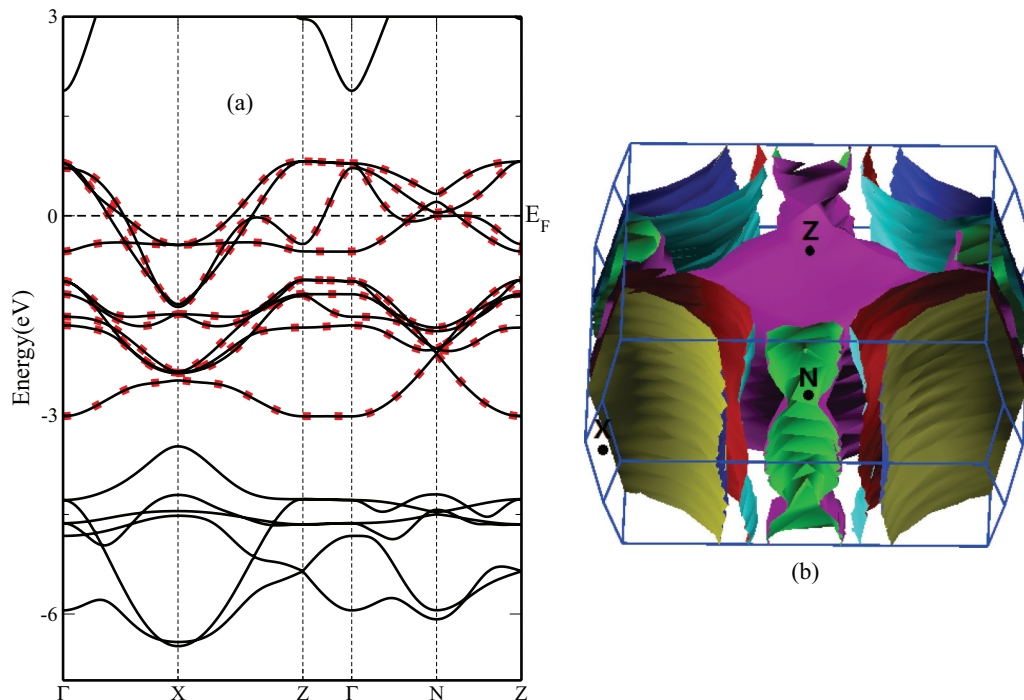


FIG. 2. (Color online) (a) Energy band structure of KNi_2S_2 by DFT (black line) and Wannier function (dotted line). (b) The Fermi surface of KNi_2S_2 by DFT calculation.

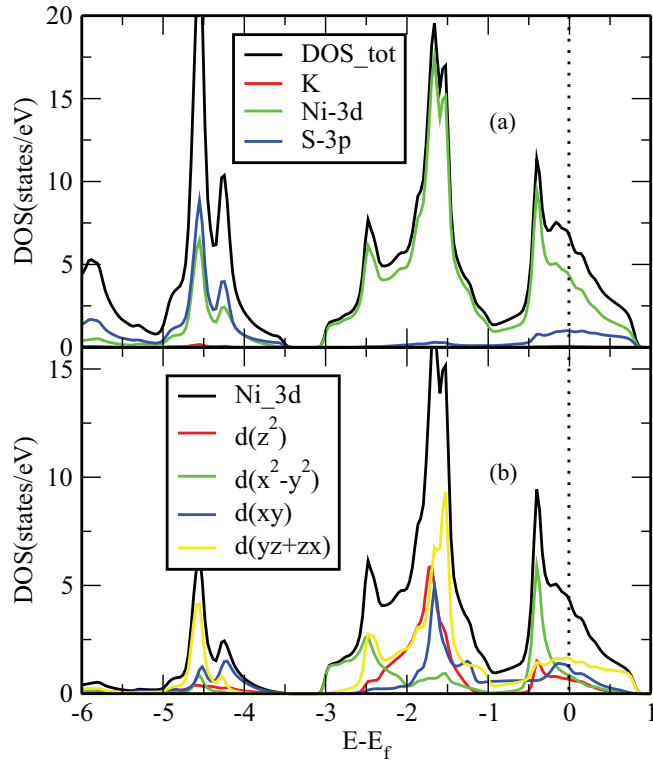


FIG. 3. (Color online) (a) DOS and PDOS of KNi_2S_2 . (b) PDOS of KNi_2S_2 for the five Fe-3d orbitals.

higher due to the higher electron count. As shown by the DOS in Fig. 3(a), the total DOS near the E_f is mainly contributed by the Ni-3d orbitals, which mix with the S-3p orbitals near the E_f . In detail, the PDOS of the Ni-3d orbitals consist of the DOS from -3 eV to 1 eV around the E_f , and at the same time there is some contribution from S-3p orbitals. Evidently, the contribution of S-3p orbitals is smaller than that from the Ni-3d orbitals. The value of the DOS at the Fermi energy $N(E_f)$ is about 6.9 states per eV per formula unit for both spins.

As we know, both LDA and GGA fail to depict the strongly correlated electron systems due to the insufficient treatment of electron correlation. In the last 20 years, many new methods and new computational tools have been developed to improve the calculation of strongly correlated electron materials, such as the DFT + U ,³⁰ DFT + DMFT (dynamical mean-field theory),³¹ and DFT + G (Gutzwiller method).¹⁸ Among all these methods, DFT + G is thought to be practically efficient and it can capture the key feature of the correlation effect as well in the ground-state studies. The Gutzwiller variational approach³² was first introduced by Gutzwiller and has been proved to be quite efficient and accurate for the ground-state physical properties studies, such as the Mott transition, ferromagnetism, and superconductivity.^{18,32-35} In our calculation, we also use the DFT + G framework to treat the correlation effects between the localized d electrons. In other words, we first construct the multiorbital Hubbard model and then solve this model with the Gutzwiller variational approach (GW). First, the Wannier function is constructed by the maximally localized Wannier functions (MLWFs) approach,³⁶ as shown by the dotted line in Fig. 2(a). Second, combined with

the Coulomb interaction, the multiorbital model can effectively describe the multiorbital characters of KNi_2S_2 . Then the GW method is used to deal with this many-body model and the physical properties in this system.^{18,32-35}

We start from this five-orbital Hubbard model,

$$H_{\text{tot}} = H_{\text{wannier}} + H_{\text{int}}, \quad (1)$$

$$H_{\text{wannier}} = \sum_{(i,j),\alpha,\beta\sigma} t_{\alpha\beta}^{ij} c_{i\alpha\sigma}^\dagger c_{j\beta\sigma},$$

$$H_{\text{int}} = U \sum_{i\alpha} n_{i\alpha\uparrow} n_{i\alpha\downarrow} + \frac{U'}{2} \sum_{i,\alpha\neq\beta,\sigma,\sigma'} n_{i\alpha\sigma} n_{i\beta\sigma'} - \frac{J}{2} \sum_{i,\alpha\neq\beta,\sigma} n_{i\alpha\sigma} n_{i\beta\sigma}, \quad (2)$$

where $c_{i\alpha\sigma}^\dagger$ ($c_{i\alpha\sigma}$) is the creation (annihilation) operator of the electron at site i with orbital α and spin σ ($=\uparrow, \downarrow$), and $n_{i\alpha\sigma}$ is the electron number operator. $t_{\alpha\beta}^{ij}$ denotes the hopping integral from the β orbital at site j to the α orbital at site i . H_{wannier} describes the on-site energies and hopping integrals of electrons between the Ni-3d Wannier orbitals, and H_{int} is the local interaction term for the Coulomb interaction between the d electrons described by the parameters U , U' , J . The parameters U , U' , and J denote the intraorbital Coulomb interaction, interorbital Coulomb interaction, and Hund's coupling. In what follows, considering the realistic wave functions of 3d orbitals³⁷ and the spin rotational symmetry, we adopt the relationship $U = U' + 2J$.

The true ground state of H_{tot} is described by the Gutzwiller wave function $|\Psi_G\rangle$, which is constructed by a many-particle projection operator \hat{P}_G on the uncorrelated wave function $|\Psi_0\rangle$,

$$|\Psi\rangle = \hat{P}_G |\Psi_0\rangle = \prod_i \hat{P}_i |\Psi_0\rangle, \quad (3)$$

with Gutzwiller projector operator

$$\hat{P}_i = \sum_{\Gamma} \lambda_{\Gamma} |\Gamma\rangle \langle \Gamma|, \quad (4)$$

where λ_{Γ} is the variational parameter for the i th site with the atomic eigenstates $|\Gamma\rangle$, which is determined by minimizing the ground-state total energy. The renormalization of the kinetic energy can be described by the bandwidth renormalization or quasiparticle weight factor Z , as defined in Ref. 17.

Generally speaking, the essence of the correlation effects under the Gutzwiller approach is to suppress the double occupancy and to renormalize the kinetic energy. Specifically, the Coulomb interaction U' will enhance the orbital polarization; however, the interorbital Hund's coupling J favors even distribution of electrons among five orbitals. To understand the role of Coulomb interaction and the change of the band structure in the presence of interactions, the value of the quasiparticle weight factor Z of the kinetic energy as a function of U at fixed $J = 0.8$ eV is shown in Fig. 4. As shown by the solid line in Fig. 4(a), the Z factor decreases with the increase of the Coulomb interaction U , due to the suppression of the double occupancy by U . Because of the valence state of $\text{Ni}^{1.5+}$, every five Ni-3d orbitals have 8.5 electrons and are noninteger filling. Thus, the metal insulator transition does not

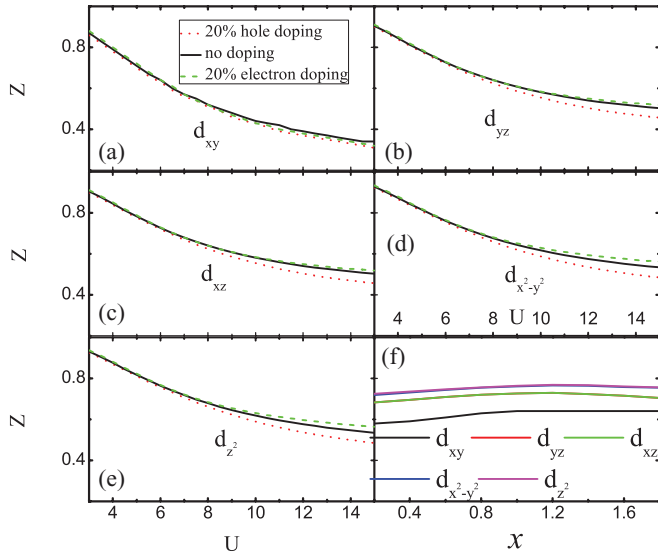


FIG. 4. (Color online) The quasiparticle weight factor Z as a function of Coulomb interaction U at $J = 0.8$ eV. The quasiparticle weight factor Z for (a) d_{xy} orbital, (b) d_{yz} orbital, (c) d_{xz} orbital, (d) $d_{x^2-y^2}$ orbital, (e) d_{z^2} orbital, and (f) as a function of doping x for KNi_2S_2 at $U = 8$ eV and $J = 0.8$ eV.

occur in this system and KNi_2S_2 is a multiorbital metal system, which is in agreement with experiment.¹⁶ In the iron-based or the copper-based superconductors, different doping with holes (p type) or electrons (n type) has an important influence on the superconducting transition temperature, which leads to a rich phase diagram of these high-temperature superconductors. For example, superconductivity only occurs in a doping range, which indicates that electron doping or hole doping may affect the electronic properties in these materials. To study the doping effect on the physical properties of KNi_2S_2 , we investigate the quasiparticle weight factor Z at different doping situations, as shown in Figs. 4(a)–4(e). The dotted line shows Z at the 20% hole doping, the black solid line shows Z without doping, and the dashed line shows Z at the 20% electron doping. When the Coulomb interaction U is not too large, the electron or hole doping almost do not affect the quasiparticle weight factor Z . But, the difference of the quasiparticle weight factor Z with different doping become more and more obvious with the increase of the U in the large range, and the value of Z is also dependent on the orbital degree of freedom due to the orbital anisotropy. For example, the doping effect is very weak for the d_{xy} orbital but important for the d_{z^2} orbital in the large- U range, as shown in Figs. 4(a)–4(e). At fixed Coulomb interaction value $U = 7$ eV, $J = 0.8$ eV, the variation of the quasiparticle weight factor Z with different doping is also investigated and plotted in Fig. 4(f). The results show that the correlated electron character of the KNi_2S_2 has been maintained with the electron-like or hole-like doping for all the Ni-3d orbitals, which is in good agreement with the experimental measurements.³⁸

The corresponding band structures and PDOS of the Ni-based superconducting compound KNi_2S_2 calculated by the GW method are presented in Fig. 5 and Fig. 6. Since the electron occupation number is 8.5 for each Ni-3d orbital and the five Ni-3d orbitals are almost occupied by the electrons, the

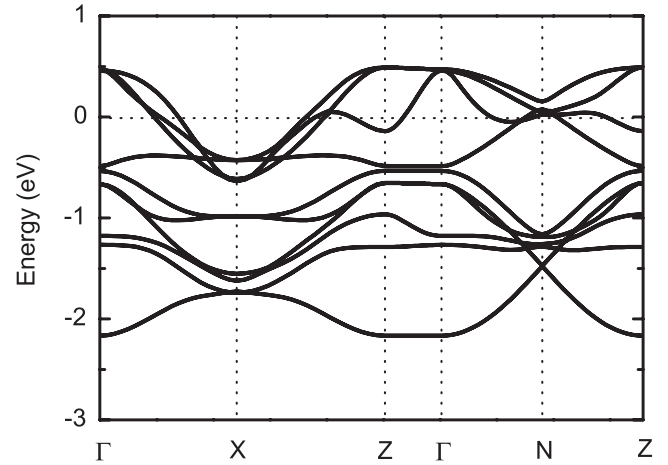


FIG. 5. Electronic band structure of KNi_2S_2 calculated with the Gutzwiller method.

added Coulomb interactions cannot make KNi_2S_2 become a Mott insulator state, which is in agreement with experiment.¹⁶ At a typical value of Coulomb interaction $U = 8$ eV and $J = 0.8$ eV,^{39–41} the quasiparticle weight factor is about 0.5. In other words, the overall bandwidth calculated by the GW method is smaller than that by the DFT calculation due to the strong correlation effect among the Ni-3d orbital electrons. In the DFT results, the band structure near the Fermi level along the X-Z line is very simple, which causes a two-FS structure along the X-Z line. Actually, our GW calculation shows that there are three Bloch bands across the Fermi level along the X-Z line due to the existence of the correlation effect, which would induce a very complicated FS along the X-Z line. The corresponding electron FS will dominate the low-energy properties along the X-Z line, which is easier to be observed with angle-resolved photoemission spectroscopy experiments (ARPES). As shown above, comparing with the DFT calculation, the GW calculation can improve the correct band narrowing and mass renormalization, which can also be seen from the DOS calculated with the DFT + G method,

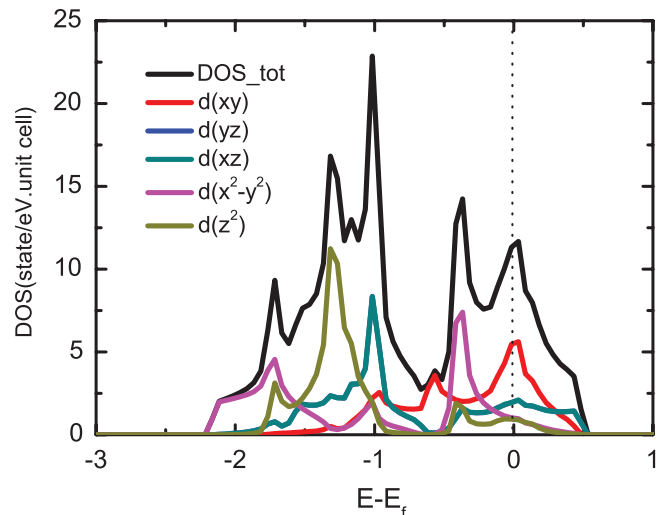


FIG. 6. (Color online) DOS and PDOS of KNi_2S_2 calculated with the Gutzwiller method.

as shown in Fig. 6. The corresponding orbital character is also plotted in Fig. 6. Comparing the orbital character of the Ni-based superconductor with that of the iron-based superconductor,¹⁹ we can clearly find that all the Ni-3*d* orbitals are renormalized by the correlation effect. We obtain the value of the DOS at the Fermi energy $N(E_f)$ of about 11.5 states per eV per formula unit for both spins, which corresponds to a bare specific-heat coefficient $\gamma = 27$ mJ mol f.u.⁻¹ K⁻² based on the formula $\gamma = \pi^2 k^2 N(E_f)/3$.^{42,43} This γ value is 2.5 times smaller than the experimental value $\gamma = 68$ mJ mol f.u.⁻¹ K⁻²,¹⁶ but it is better than that of the DFT calculation, $\gamma = 16.2$ mJ mol f.u.⁻¹.

IV. CONCLUSIONS

In conclusion, we have presented the results of the electronic structure of KNi₂S₂ based on DFT plus Gutzwiller variational calculations. The results show that the ground state of KNi₂S₂ is a strongly correlated metal and the energy bands near Fermi level are dominated by the Ni-3*d* electron states. The multiorbital correlation effect between the Ni-3*d* electrons determines the main physical properties of newly discovered Ni-based superconductor KNi₂S₂, such as the mass enhancement behavior and the multiorbital characters. Different from the DFT understanding, the band structure

has many changes under the correlation effect, especially for the band structure along the X-Z high-symmetry line. In particular, the bands are narrowed by a factor of about 2, and all the five Ni-3*d* orbitals are almost filled, which determines the low-energy physical properties of KNi₂S₂. The calculation about the electronic structure provides a reasonable starting point for the investigations of the Ni-based superconductor. The variation of the quasiparticle weight factor with the doping is also investigated and compared to the experiments. Our results confirm that KNi₂S₂ is a multiorbital strongly correlated system with a reduced renormalized bandwidth by the correlation effect.

ACKNOWLEDGMENTS

The authors thank X. Dai for helpful discussions. F.L. wishes to acknowledge the partial support of HKU UDF-CSE. F.C.Z. acknowledges the support of RGC HKU707211 and AOE/P-04/08. W.H.W. acknowledges the support of the NSFC (Grants No. 11104148 and No. 11047162), Tianjin Key Technology R&D Program (Grant No. 11ZCKFGX01300), the Specialized Research Fund for the Doctoral Program of Higher Education (Grants No. 20100031120035 and No. 20110031110034), and Fundamental Research Funds for the Central Universities.

¹Y. Kamihara, T. Watanabe, M. Hirano, and H. Hosono, *J. Am. Chem. Soc.* **130**, 3296 (2008).

²G. F. Chen, Z. Li, G. Li, J. Zhou, D. Wu, J. Dong, W. Z. Hu, P. Zheng, Z. J. Chen, H. Q. Yuan, J. Singleton, J. L. Luo, and N. L. Wang, *Phys. Rev. Lett.* **101**, 057007 (2008).

³H. Lei, M. Abeykoon, E. S. Bozin, K. Wang, J. B. Warren, and C. Petrovic, *Phys. Rev. Lett.* **107**, 137002 (2011).

⁴S. Yang, W. L. You, S. J. Gu, and H. Q. Lin, *Chin. Phys. B* **18**, 2545 (2009).

⁵G. Wu, Y. L. Xie, H. Chen, M. Zhong, R. H. Liu, B. C. Shi, Q. J. Li, X. F. Wang, T. Wu, Y. J. Yan, J. J. Ying, and X. H. Chen, *J. Phys.: Condens. Matter* **21**, 142203 (2009).

⁶J. G. Guo, S. F. Jin, G. Wang, S. C. Wang, K. X. Zhu, T. T. Zhou, M. He, and X. L. Chen, *Phys. Rev. B* **82**, 180520(R) (2010).

⁷M. H. Fang, H. D. Wang, C. H. Dong, Z. J. Li, C. M. Feng, J. Chen, and H. Q. Yuan, *Europhys. Lett.* **94**, 27009 (2011).

⁸H. D. Wang, C. H. Dong, Z. J. Li, S. S. Zhu, Q. H. Mao, C. M. Feng, H. Q. Yuan, and M. H. Fang, *Europhys. Lett.* **93**, 47004 (2011).

⁹T. Qian, X.-P. Wang, W.-C. Jin, P. Zhang, P. Richard, G. Xu, X. Dai, Z. Fang, J.-G. Guo, X.-L. Chen, and H. Ding, *Phys. Rev. Lett.* **106**, 187001 (2011).

¹⁰W. Bao, Q. Z. Huang, G. F. Chen, M. A. Green, D. M. Wang, J. B. He, and Y. M. Qiu, *Chin. Phys. Lett.* **28**, 086104 (2011).

¹¹F. Ye, S. Chi, W. Bao, X. F. Wang, J. J. Ying, X. H. Chen, H. D. Wang, C. H. Dong, and M. H. Fang, *Phys. Rev. Lett.* **107**, 137003 (2011).

¹²W. Bao, G. N. Li, Q. Huang, G. F. Chen, J. B. He, M. A. Green, Y. Qiu, D. M. Wang, and J. L. Luo, *Physica C* **474**, 1 (2012).

¹³P. A. Lee, N. Nagaosa, and X. G. Wen, *Rev. Mod. Phys.* **78**, 17 (2006).

¹⁴L. Ma, A. Q. Huang, and J. Li, *Chin. Phys. B* **20**, 037104 (2011).

¹⁵J. R. Neilson, A. Llobet, A. V. Stier, L. Wu, J. Wen, J. Tao, Y. Zhu, Z. B. Tesanovic, N. P. Armitage, and T. M. McQueen, *Phys. Rev. B* **86**, 054512 (2012).

¹⁶J. R. Neilson, T. M. McQueen, A. Llobet, J. Wen, and M. R. Suchomei, *Phys. Rev. B* **87**, 045124 (2013).

¹⁷V. V. Bannikov and A. L. Ivanovskii, arXiv:1302.1661.

¹⁸X. Y. Deng, L. Wang, X. Dai, and Z. Fang, *Phys. Rev. B* **79**, 075114 (2009).

¹⁹G. T. Wang, Y. M. Qian, G. Xu, X. Dai, and Z. Fang, *Phys. Rev. Lett.* **104**, 047002 (2010).

²⁰P. Giannozzi *et al.*, *J. Phys.: Condens. Matter* **21**, 395502 (2009).

²¹J. P. Perdew, K. Burke, and M. Ernzerhof, *Phys. Rev. Lett.* **77**, 3865 (1996).

²²D. Vanderbilt, *Phys. Rev. B* **41**, 7892 (1990).

²³I. I. Mazin, D. J. Singh, M. D. Johannes, and M. H. Du, *Phys. Rev. Lett.* **101**, 057003 (2008).

²⁴D. J. Singh and M. H. Du, *Phys. Rev. Lett.* **100**, 237003 (2008).

²⁵L. Boeri, O. V. Dolgov, and A. A. Golubov, *Phys. Rev. Lett.* **101**, 026403 (2008).

²⁶C. Cao, P. J. Hirschfeld, and H. P. Cheng, *Phys. Rev. B* **77**, 220506(R) (2008).

²⁷F. J. Ma and Z. Y. Lu, *Phys. Rev. B* **78**, 033111 (2008).

²⁸F. Lu and L. J. Zou, *J. Phys.: Condens. Matter* **22**, 355603 (2010).

²⁹X. W. Yan, M. Gao, Z. Y. Lu, and T. Xiang, *Phys. Rev. B* **84**, 054502 (2011).

³⁰V. I. Anisimov, J. Zaanen, and O. K. Andersen, *Phys. Rev. B* **44**, 943 (1991).

³¹G. Kotliar, S. Y. Savrasov, K. Haule, V. S. Oudovenko, O. Parcollet, and C. A. Marianetti, *Rev. Mod. Phys.* **78**, 865 (2006).

- ³²M. C. Gutzwiller, *Phys. Rev. Lett.* **10**, 159 (1963).
- ³³D. Vollhardt, *Rev. Mod. Phys.* **56**, 99 (1984).
- ³⁴W. F. Brinkman and T. M. Rice, *Phys. Rev. B* **2**, 4302 (1970).
- ³⁵F. C. Zhang, C. Gros, T. M. Rice, and H. Shiba, *Supercond. Sci. Technol.* **1**, 36 (1988).
- ³⁶M. Nicola, A. M. Arash, R. Y. Jonathan, S. Ivo, and V. David, *Rev. Mod. Phys.* **84**, 1419 (2012).
- ³⁷C. Castellani, C. R. Natoli, and J. Ranninger, *Phys. Rev. B* **18**, 4945 (1978).
- ³⁸H. C. Lei, K. F. Wang, H. J. Ryu, D. Graf, J. B. Warren, and C. Petrovic, [arXiv:1211.1371](https://arxiv.org/abs/1211.1371).
- ³⁹F. Lu, J. Z. Zhao, and W. H. Wang, *J. Phys.: Condens. Matter* **24**, 495501 (2012).
- ⁴⁰M. K. Stewart, J. Liu, M. Kareev, J. Chakhalian, and D. N. Basov, *Phys. Rev. Lett.* **107**, 176401 (2011).
- ⁴¹M. J. Han, X. Wang, C. A. Marianetti, and A. J. Millis, *Phys. Rev. Lett.* **107**, 206804 (2011).
- ⁴²David J. Singh, *Phys. Rev. B* **86**, 174507 (2012).
- ⁴³Paul A. Beck and Helmut Claus, *J. Res. Natl. Bur. Stand., Sect. A* **74**, 449 (1970).